Negative Differential Resistance (NDR) Frequency Conversion with Gain

R. J. Hwu, R. W. Alm, and S. C. Lee
Department of Electrical Engineering
University of Utah

Abstract--The dependence of the I-V characteristic of the negative differential resistance (NDR) devices on the power level and frequency of the rf input signal has been theoretically analyzed with a modified large- and small-signal nonlinear circuit analysis program [1,2]. The NDR devices we used in this work include both the tunnel diode (without the antisymmetry in the I-V characteristic) and resonant-tunneling devices (with the antisymmetry in the I-V characteristic). Absolute negative conductance can be found from a zero-biased resonant tunneling device when the applied pump power is within a small range. This study verifies the work of Sollner et al. [3]. Variable negative conductances at the fundamental and harmonic frequencies can also be obtained from both the unbiased and biased tunnel diodes. The magnitude of the negative conductances can be adjusted by varying the pump amplitude--a very useful circuit property. However, the voltage range over which the negative conductance occurs moves towards the more positive side of the voltage axis with increasing frequency. Furthermore, the range of the pumping amplitude to obtain negative conductance varies with the parasitics (resistance and capacitance) of the device. The theoretical observation of the dependence of the I-V characteristic of the NDR devices on the power and frequency of the applied pump signal is supported by the experimental results. In addition, novel functions of a NDR device such as self-oscillating frequency multiplier and mixer with gain have been experimentally demonstrated. The unbiased oscillator have also been successfully realized with a NDR

device with an antisymmetrical I-V characteristic. Finally, the applications of these device functions will be discussed.

INTRODUCTION

There have been increased interest in the study of resonant tunneling devices due to the fact that the characteristics of these devices can be engineered to have properties for very high-speed applications. In particular, their ability to exhibit negative differential resistance (NDR) regions lead to their potential use as gain elements in circuits and offers a new opportunity for circuit design. The presence of peaks and valleys in the I-V curve combined with the overall antisymmetry of the I-V curve about the origin [i.e., I(V) = -I(-V)], also offers the potential for efficient odd-harmonic generation with an unbiased resonant tunneling device [4,5]. The key lies in pumping the device so that the peak amplitude of the voltage across the device occurs above the resonant current peaks. This will produce more than three local maxima in the device current waveform over one cycle, corresponding to third or higher odd harmonic generation. The resonant tunneling frequency multiplier, therefore, has several distinct advantages over existing resistive multipliers, which are usually based on Schottky barrier diodes. The antisymmetrical response provides the potential for efficient odd harmonic frequency multiplication with an unbiased resonant tunneling device due to cancellation of the even harmonics, therefore greatly simplifying the circuit design. The maximum harmonic generation efficiency of a resonant tunneling device is significantly higher than the $1/n^2$ (n is the harmonic number) value that applies to standard resistive multipliers because of its negative resistance [4,5] (i.e., nonmonotonically increasing function I-V characteristic). The resonant tunneling device also has the ability to act as an efficient mixer due to the rapid variation of the dynamic conductance with voltage near the NDR region of the I-V curve. The resonant tunneling mixer has the potential to displace the Schottky diode in many microwave and millimeter-wave applications. The most intriguing aspect of the resonant tunneling frequency multiplier and mixer is its intrinsic capability to achieve conversion gain (efficiency > 1).

LARGE- AND SMALL-SIGNAL NONLINEAR-CIRCUIT ANALYSIS

A large- and small-signal analysis program has been developed to analyze the behavior of dc and microwave negative conductance of a NDR device. The analysis technique was developed by T. Kerr [6] and the computer program was implemented for analyzing ideal Schottky barrier diodes by Siegel et. al. [1]. The analysis program has been modified to take into account the negative resistance of the NDR device [2]. The I-V characteristics measured from the NDR devices as can be seen in Fig. 1 have been used in the nonlinear-circuit analysis. Since the devices were mounted on a 50 Ω microstrip line for the measurements in this work, the embedding impedance of 50 Ω at every harmonic frequency has been used. A simple experiment has been carried out to verify that the embedding impedance at higher harmonic frequencies is equal to 50 Ω [7].

Tunnel Diode--Without Antisymmetry in the I-V Characteristic

The differential conductance of a tunnel diode biased at zero voltage and in the positive differential resistance (PDR) region (close to the current peak) under different rf pumping conditions has been studied in this work. No negative conductance has been observed at dc for a tunnel diode biased at zero voltage and in the PDR region. However, negative conductances at the fundamental and different harmonic frequencies have been observed from a tunnel diode biased at zero voltage and in the PDR region. The magnitude of the negative conductance varies with the pump amplitude (see Fig. 2). The pump amplitude region required to achieve the negative conductance moves toward the more positive side of the power axis with increasing pumping frequency (also see Fig. 2). This can be easily explained using the equivalent circuit model of a tunnel diode (see Fig. 1 (c)). Since the impedance of the parallel circuit section decreases with the increasing frequency, more voltage will be distributed on the series resistance and less voltage on the parallel circuit section for the higher pumping frequency. The negative conductance observed at the fundamental and different harmonic frequencies can be used as the basis for harmonic oscillators. It should be pointed out that the magnitude of the negative conductance at the fundamental is much higher than those at other harmonic frequencies with a tunnel diode biased in the PDR region, close to the current peak (see Fig. 2 (b) and (c)). At this bias point, near the region of greatest curvature, the Fourier series of the conductance waveform has a predominant coefficient at the oscillation frequency. In addition, the negative conductances at the odd harmonic frequencies are higher than those at the even harmonic frequencies for the tunnel diode biased in the PDR region, close to the current peak due to the antisymmetrical conductance-voltage (G-V) characteristic at this bias point. The power levels at which the maximum negative conductances at the fundamental and second harmonic frequency occur are smaller than those for a unbiased tunnel diode.

The differential conductance of a tunnel diode biased at the center of the NDR region has also been studied. From the results shown in Fig. 3 (a), an absolute negative conductance to dc has been obtained from a tunnel diode biased in the NDR region when the applied pump amplitude is within a small range. That is, the conductance of the resonant tunneling device will be negative at any frequency when the pump amplitude is within this small range. The value of the absolute negative conductance is approximately the same as that found in the NDR region. The magnitude of the negative conductances changes with the pumping power level (see Fig. 3). That the absolute negative conductance occurs for the tunnel diode biased in the NDR region asserts that oscillation can occur at any frequency if the pumping power is within the region that the negative conductance occurs. The magnitude of the negative conductance at the second harmonic is higher than those at dc, the fundamental and third harmonic frequencies due to the symmetrical G-V characteristic at this bias point (see Fig. 3 (b)). The variable absolute negative conductance observed can be used as the basis for oscillators and harmonic oscillators up to the cut-off frequency of the diode. The self-oscillation capability of a tunnel diode biased in the NDR region can, therefore, finds applications as biased self-oscillating mixers and frequency multipliers. The self-oscillating frequency multiplier and mixer discussed here do not require a large-signal rf pump.

It should be noted that the self-oscillation at the fundamental generates its own harmonics using the nonlinearity of the NDR device; this will be referred to as the self-oscillating frequency multiplier. While the harmonic oscillator refers to the case that the NDR device oscillates at a particular harmonic frequency using the negative conductance at that harmonic frequency. It should be pointed out that the conversion gain (efficiency > 1) can be achieved from the biased self-oscillating frequency multiplier and mixer.

Resonant Tunneling Device--With Antisymmetry in the I-V Characteristic

From the nonlinear-circuit analysis results, an absolute negative conductance to dc can be found from a resonant tunneling device at zero bias when the applied pump power is within a small range (see Figs. 4 (a) and (b)). The value of the negative conductance is approximately the same as that found in the NDR region. As can be seen from the results in Figs. 4 (a) and (b), the magnitude of the negative conductance can be adjusted by varying the pump amplitude. This study verifies the work of Sollner et al. [3]. However, the voltage range over which the negative conductance occurs is strongly dependent on the pumping frequency. This region moves towards the more positive side of the power axis when the pumping frequency increases (see Figs. 4 (a) and (b)). The reason for this can, again, be explained with a equivalent circuit model (discussed for the tunnel diode in previous section).

We found that the range of the applied pump power to obtain absolute negative conductance varies with the parasitics (series resistance and capacitance) of the device. As can be seen from Fig. 5, the pumping power region over which the negative conductance occurs move towards the more positive side of the power axis with increasing capacitance and series resistance of the device. This again can be seen from the equivalent circuit model of a NDR diode. When the series resistance and/or capacitance of the device increases, more voltage drops across the series resistance and, therefore, less power is developed across the parallel circuit section of the equivalent circuit. It should be pointed out that the dependence of the conductance on the parasitics of the device is similar to that on the rf input frequency.

The conductance of the resonant tunneling diode will be negative at any frequency when the pump amplitude is within a small range. Figures 4 (c) and (d) show the differential conductance at the second harmonic frequency versus pumping power and pump amplitude, respectively. The magnitude of the negative conductance at the second harmonic frequency is larger than the negative conductances at dc and at fundamental frequency. This is due to the symmetrical G-V characteristic of the resonant tunneling device. The variable absolute negative conductance observed can be used for oscillators up to the cut-off frequency of the diode.

From these studies, one can expect to find absolute negative resistance whenever a material with negative differential conductance and an I-V curve that is antisymmetrical is driven with a pump of the right amplitude and frequency. The resonant tunneling device can also perform the same functions such as the self-oscillating frequency multiplier and mixer discussed for a tunnel diode if it is biased in the NDR region. It should be pointed out that the biased tunnel and resonant tunneling device (in the PDR region) requires less pumping power to achieve self-oscillation than the unbiased device. The biased self-oscillation tunnel diode and resonant tunneling frequency multipliers and mixers have the intrinsic capability of conversion gain. For the unbiased oscillator operations, it should be noted that little in the way of negative conductance or dynamic range has been sacrificed with this operation, and the advantage of operating with zero DC bias voltage has been gained. It should be further noted that the increase in negative conductance at a specific frequency (depending upon the operating point) could simplify frequency selection for oscillator designs.

EXPERIMENTAL RESULTS

During the experimental measurements, it was observed that the dc I-V characteristic of the NDR device is very strongly dependent on the power level of the rf input signal. The dc I-V characteristics of the NDR devices (with and without the antisymmetrical I-V characteristics) measured at different rf input power levels are shown in Figs. 6 and 7, respectively. The dc I-V characteristics of the tunnel diode measured at different rf input frequencies are shown in Fig. 8. Based on these results, the dc I-V characteristics of the NDR device changes dramatically with the increasing input power level and frequency. The dependence of the I-V characteristics of the NDR device on the frequency of the rf input signal can easily be seen from the equivalent circuit model of the NDR device. The frequency dependence of the impedance across the parallel circuit section of the equivalent circuit results in the power dependence of the I-V characteristics. The power dependence of the negative conductance complicates the dependence of the negative conductance on the frequency. The nonlinear circuit analysis was used to theoretically verify this observation. The I-V curves measured at different pumping power levels as shown in Figs. 6 and 7 and the I-V curves measured at different pumping frequencies as shown in Fig. 8 compare favorably to the simulation results.

Based upon this study, the design, operation, and performance of the NDR frequency multiplier, self-oscillating frequency multiplier and mixer and harmonic oscillator can be complicated. For a constant rf input frequency, the biasing and pumping conditions and output power of the self oscillation of the NDR device vary with the rf input power level. In addition, the onset of self oscillation of a NDR device biased in the NDR region also depends upon the rf input power level. For example, the self oscillation can be suppressed by changing the rf input power level (tuning the I-V characteristic) in the frequency multiplication operation of a NDR device. However, this will cause the conversion efficiency of the device to change as well since the nonlinearity is not the same. In addition, the self-oscillation with a constant rf input frequency may disappear for a given dc bias depending upon the rf input power level for the self-oscillating frequency multiplier, mixer and harmonic oscillator applications. Determination of the biasing and operating conditions and performance of the NDR frequency multiplier, self-oscillating frequency multiplier and mixer, and harmonic oscillator, therefore, requires complete information of the I-V characteristics at different rf input frequencies and power levels. This can be accomplished by extensive simulations of the NDR device under different pumping conditions using the modified large- and small-signal nonlinear circuit analysis program as mentioned above.

A NDR biased in the NDR region can be used for the self-oscillating frequency multiplier and mixer. Both the self-oscillating frequency multiplier and mixer have been successfully demonstrated using a tunnel diode biased in the NDR region. The results from a self-oscillating frequency multiplier can be seen in Fig. 9. The highest tripling efficiency has been obtained at the center of the NDR region while the highest doubling efficiency has been obtained at the edges of the NDR region of the tunnel diode as expected. This is due to the I-V characteristic being antisymmetrical when biased at the center of the NDR region, and the I-V characteristic being almost symmetrical when biased close to the current peak. It should be pointed out that the circuit used does not allow independent tuning of the harmonics.

APPLICATIONS

The wide use of resonant tunnel devices is limited, to a considerable extent, by the low level of their output power. Power combining techniques are employed to increase the output power of the resonant tunneling devices. The device-grid array approach is a potentially attractive way to spatially combine the output power of large numbers of resonant tunneling devices. In this approach, a grid is monolithically integrated with thousands of devices thereby overcoming the power limitations of a single device since the power is distributed among the many devices making possible watt-level CW output power throughout the microwave and millimeter-wave region [8,9]. This kind of array can find applications as a high frequency, high power solid-state rf power source. All the interconnections of the high- and low-frequency leads of each port of each device (especially, three-terminal devices) present an extremely difficult problem for the development of such arrays. The demonstration of novel unbiased oscillators is most useful for the development of monolithic planar wafer-scale device arrays since no dc bias lines are required, which greatly simplify the grid design.

In addition, the pumping power for a device grid is significantly higher than that for a single device (proportional to the number of the devices). Therefore, it is important to minimize the amount of input power required to pump each individual device. Based upon the theoretical and experimental work which have been performed in this study, the possibility of biasing a NDR diode to minimize the amount of power required to pump each individual diode into the desired operation point has been verified. The bias lines can be easily employed in the design of diode grid (two terminal device grid) to provide dc bias and minimize the required pumping power [9]. In addition, frequency multiplication and mixing with gain can be obtained from these biased NDR diodes as discussed in this paper.

CONCLUSION

This work employs a modified large- and small-signal nonlinear-circuit analysis [2] to verify the previous work of Sollner et al. using a simple mathematical model [3]. The absolute negative conductance can be obtained from an unbiased resonant tunneling device when the applied pump power is within a small region. The variable absolute negative conductance can be used as the basis for oscillators up to the cutoff frequency of the device. Furthermore, a NDR device biased in the NDR region can be used as the basis for the self-oscillating frequency multiplier and mixer. The biased self-oscillating frequency multiplier and mixer can achieve conversion gain (efficiency > 1). These functions have been experimentally demonstrated in this work. The advantage of a unbiased oscillator using a resonant tunneling device comes from the fact that the negative conductance can be adjusted by varying the pump amplitude--a very useful circuit property. In addition, the negative conductance is larger at even harmonic frequencies which could simplify frequency selection of an oscillator design based upon this effect. The advantage of operating with zero dc bias voltage is also gained. Through this study, the power dependence of the negative conductance of a NDR device on the rf input signal has been observed. The biasing and pumping conditions and performance of the frequency multiplier, self-oscillating frequency multiplier and mixer, and harmonic oscillator requires complete information of the I-V characteristics of a NDR device at different input frequencies and power levels. This information can be obtained using the modified large- and small-signal nonlinear-circuit analysis as discussed in this paper.

References

[1] H. Siegel, A. R. Kerr, and W. Hwang, "Topics in the Optimization of MM Wave Mixers," NASA Technical Paper #2287, 1987.

[2] R. J. Hwu and N. C. Luhmann, Jr., "Quantum Well Diode Frequency Multiplier Study," Second International Symposium on Space Terahertz Technology, Proceedings, pp. 226-237, 1991.

[3] T. C. L. G. Sollner, E. R. Brown, and W. D. Goodhue, Picosecond Electronics and Optoelectronics II, Editors: F. J. Leonberger, C. H. Lee, F. Capasso, and H. Morkoc, Springer-Series in Electronics and Photonics, **Vol. 24**, pp. 102-108, 1987.

[4] P. D. Batelaan and M. A. Frerking, 13th Int'l Conf. on Infrared and Millimeter Waves, Proceedings, 1988.

[5] T. C. L. G. Sollner, E. R. Brown, W. D. Goodhue, and C. A. Correa, J. Appl. Phys., **Vol. 64**, P. 4248, 1988.

[6] D. N. Held and A. R. Kerr, "Conversion Loss and Noise of Microwave and Millimeter-Wave Mixers: Part 1 - Theory," IEEE Trans. on Microwave Theory and Tech., **MTT-26**, PP. 49-55, 1978.

[7] P. P. Huang, "I-V Characterization of Negative Resistance Device by Microwave Reflection Coefficients," M.S. thesis, UCLA, pp. 49-51, 1989.

[8] D. B. Rutledge and S. E. Schwarz, "Planar Multimode Detector Arrays for Infrared and Millimeter Waves Applications," IEEE J. Quantum Electronics, **QE-17**, pp. 407-414, 1981.

[9] R. J. Hwu, C. F. Jou, N. C. Luhmann, Jr., M. Kim, W. W. Lam, Z. B. Popovic, D. B. Rutledge, "Array Concepts for Solid-State and Vacuum Microelectronics

Millimeter-Wave Generation," IEEE Trans. on Electron Device, **ED-36**, No. 11, pp. 2645-2650, 1989.

Figure Captions

Fig. 1 The I-V curves of a (a). tunnel diode and a (b). resonant tunneling device used in the nonlinear circuit analysis. (c). The equivalent circuit of a NDR device.

Fig. 2 The differential conductance of a tunnel diode biased in the PDR region (close to the current peak) at the (a). dc, (b). fundamental, and (c). third harmonic frequency from the nonlinear circuit analysis.

Fig. 3 The differential conductance of a tunnel diode biased at the center of the NDR region at the (a). dc, and (b). second harmonic frequency from the nonlinear circuit analysis.

Fig. 4 The differential conductance at dc versus (a). pump power level, and (b). pump amplitude of a zero-biased resonant tunneling device. The differential conductance at the second harmonic frequency versus (c). pump power level and (d). pump amplitude of a zero-biased resonant tunneling device from the nonlinear circuit analysis.

Fig. 5 The differential conductance at dc of a zero-biased resonant tunneling device with different (a). capacitance values of 1 pF and 1 fF with three rf input frequencies of 0.7, 12, and 90 GHz, and (b). series resistance values of 12.5 Ω, 625 Ω, and 1.25 kΩ with an rf input frequency of 0.7 GHz from the nonlinear circuit analysis.

Fig. 6 The measured I-V curves of a tunnel diode with different rf input power levels at two rf input frequencies of (a). 0.7 GHz, and (b). 2.5 GHz.

Fig. 7 The measured I-V curves of a NDR device (with an antisymmetrical I-V characteristic) with two different rf input power levels at an rf input frequency of 10 MHz.

Fig. 8 The measured I-V curves of a tunnel diode with different rf input frequencies at an rf input power level of 2 mW.

Fig. 9 The ratio of the output power to the fundamental power of a self-oscillating frequency multiplier using the tunnel diode of Fig. 6 versus different bias points in the NDR region with a rf input frequency of 0.7 GHz.

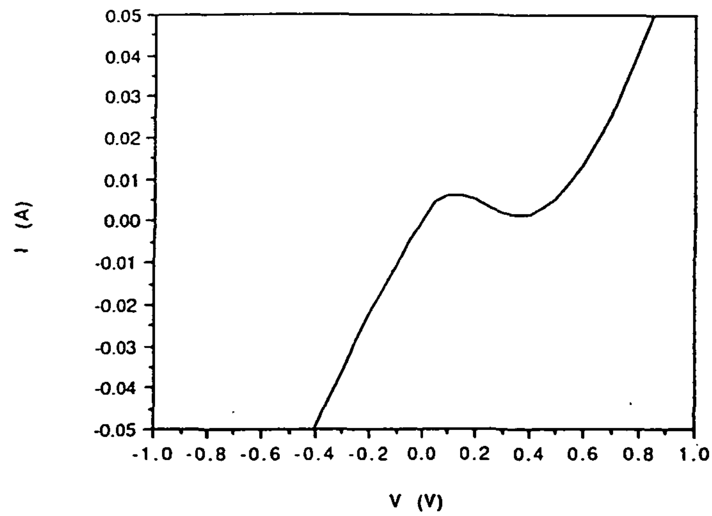

Fig. 1 (a)

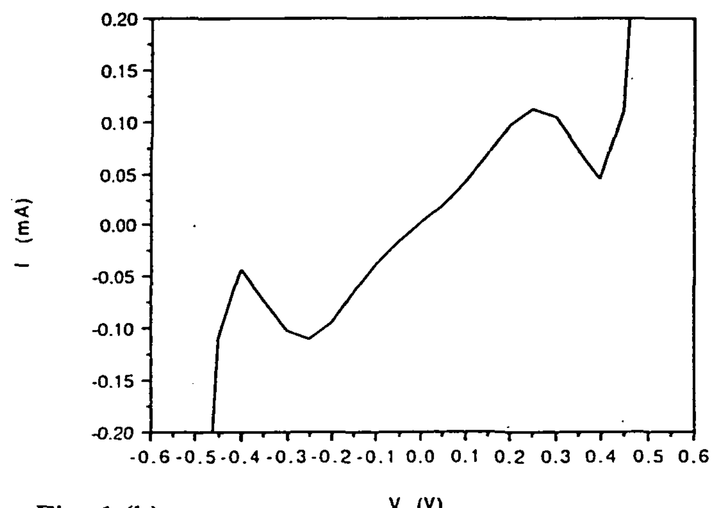

Fig. 1 (b)

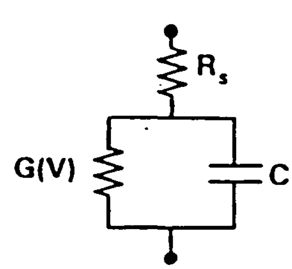

Fig. 1 (c)

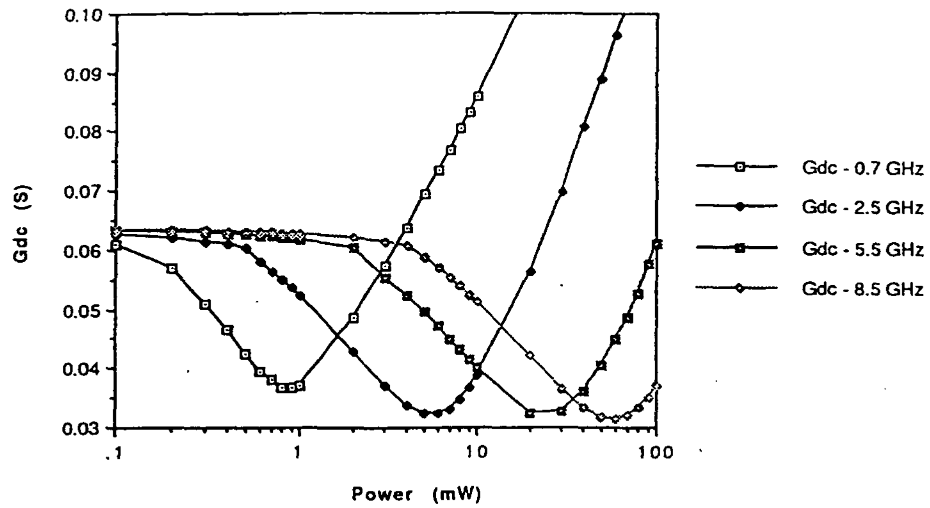

Fig. 2 (a)

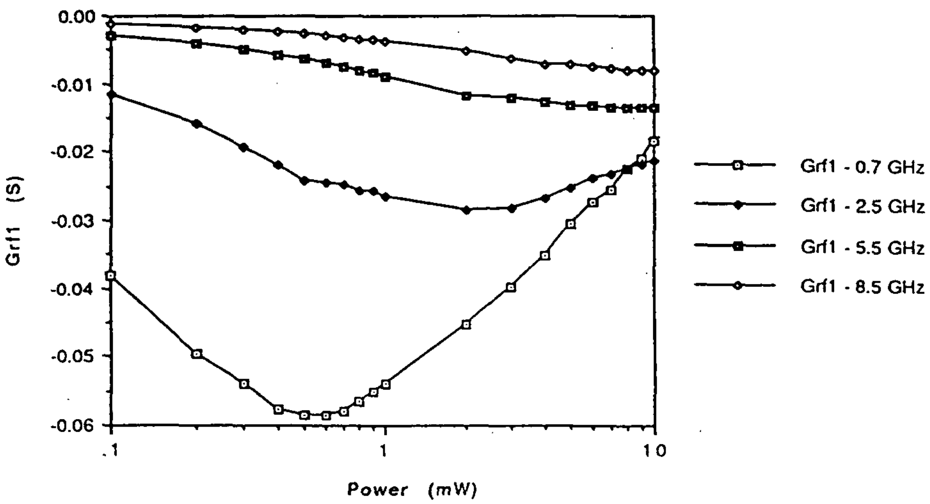

Fig. 2 (b)

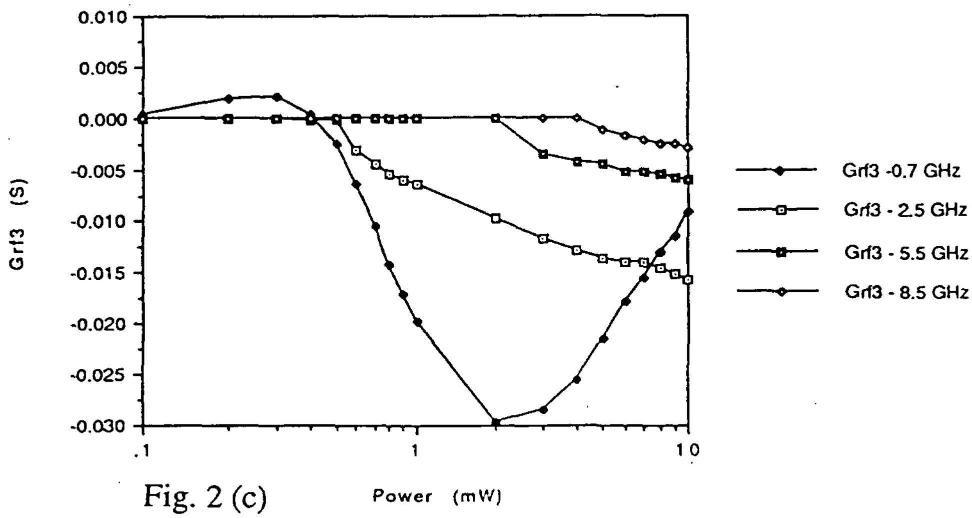

Fig. 2 (c)

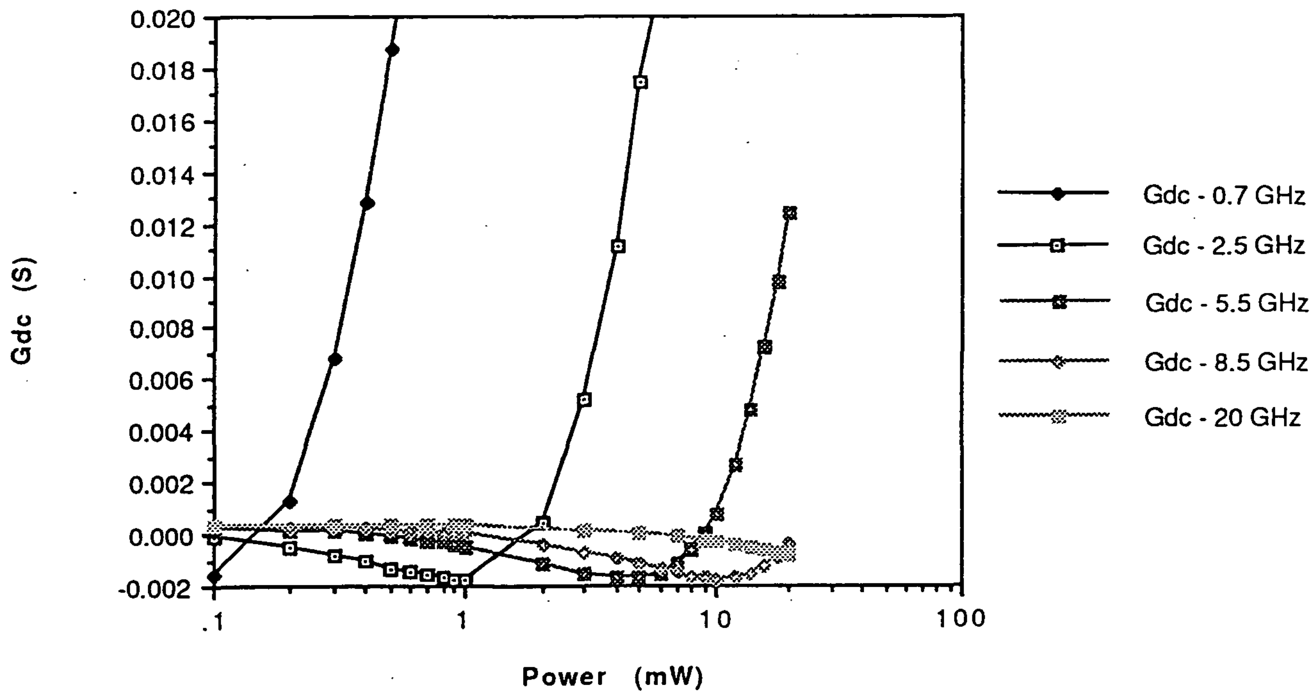
0.020
0.018
0.016
0.014
0.012
0.010
0.008
0.006
0.004
0.002
0.000
-0.002
Gdc (S)
.1
1
10
100
Power (mW)
Gdc - 0.7 GHz
Gdc - 2.5 GHz
Gdc - 5.5 GHz
Gdc - 8.5 GHz
Gdc - 20 GHz

Fig. 3 (a)

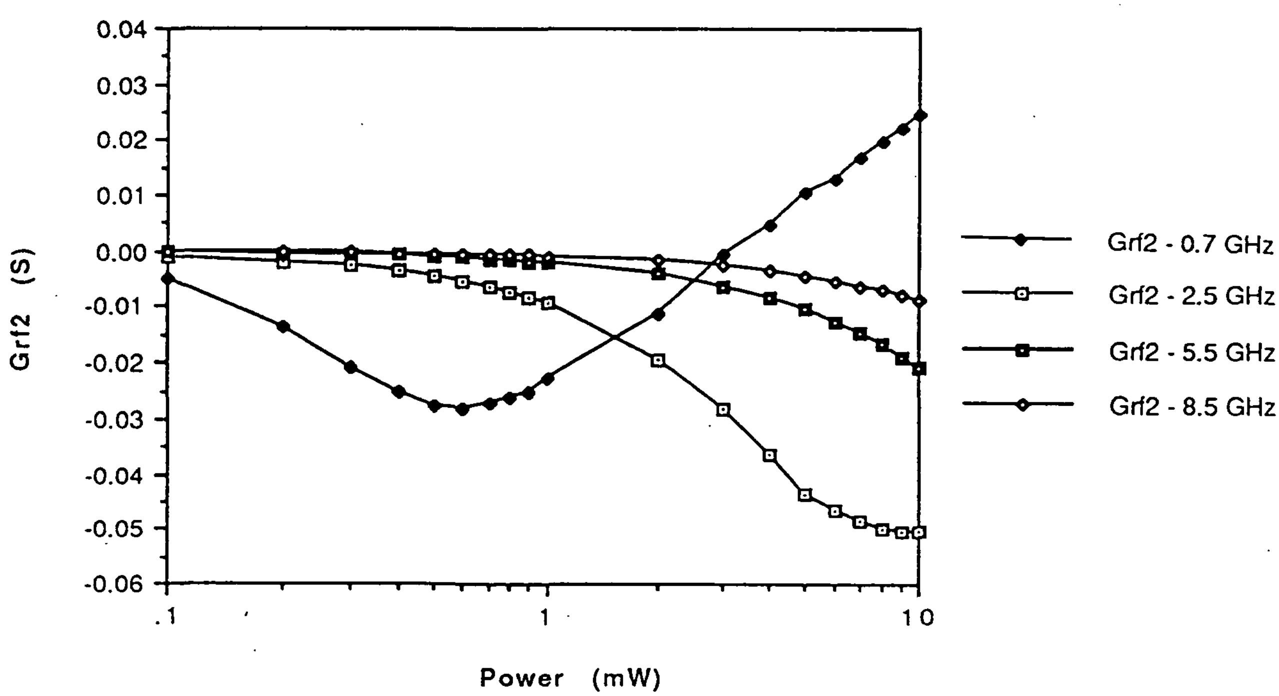
0.04
0.03
0.02
0.01
0.00
-0.01
-0.02
-0.03
-0.04
-0.05
-0.06
Grf2 (S)
.1
1
10
Power (mW)
Grf2 - 0.7 GHz
Grf2 - 2.5 GHz
Grf2 - 5.5 GHz
Grf2 - 8.5 GHz

Fig. 3 (b)

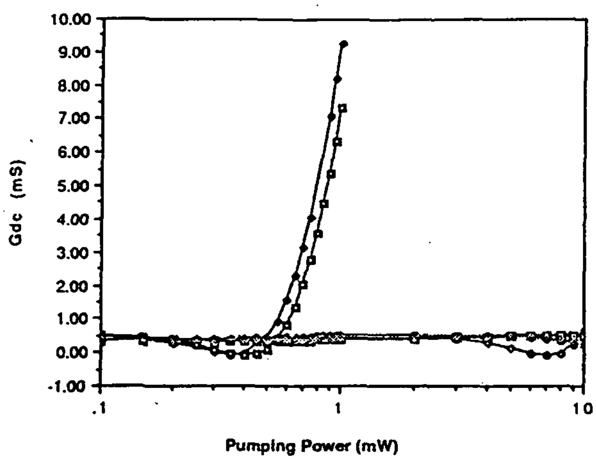

Fig. 4 (a)

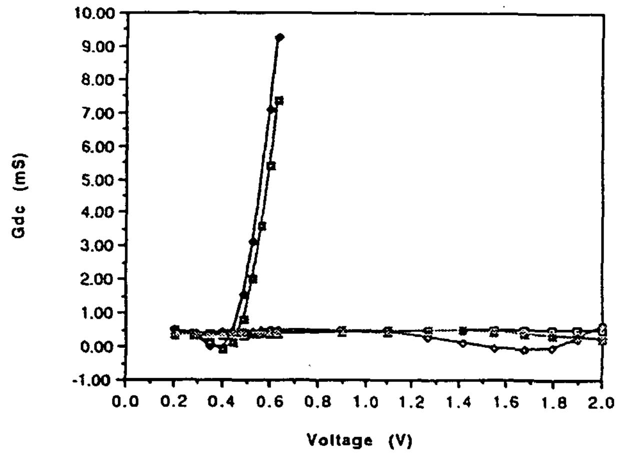

Fig. 4 (b)

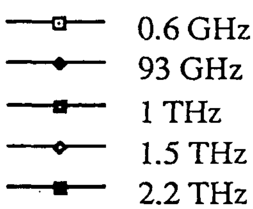

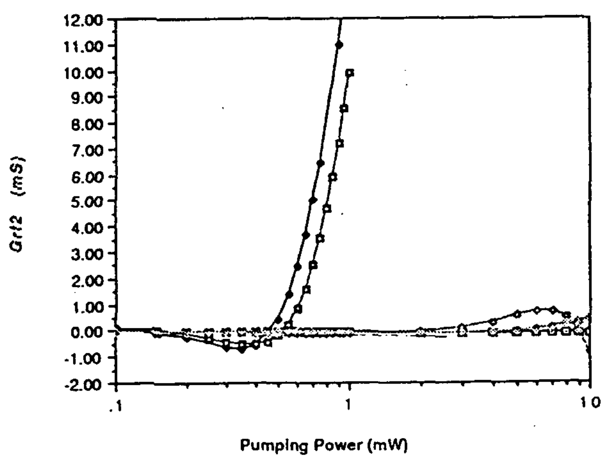

Fig. 4 (c)

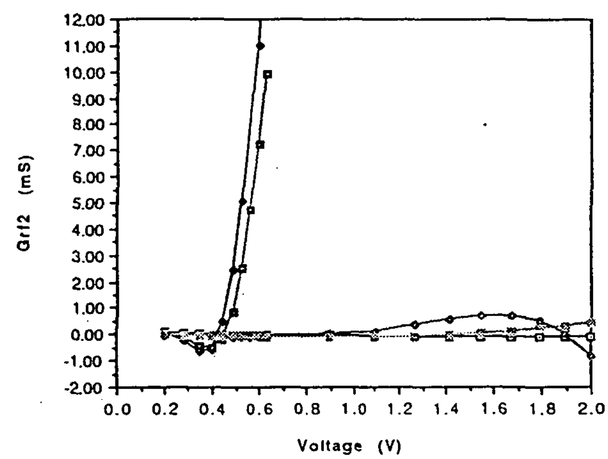

Fig. 4 (d)

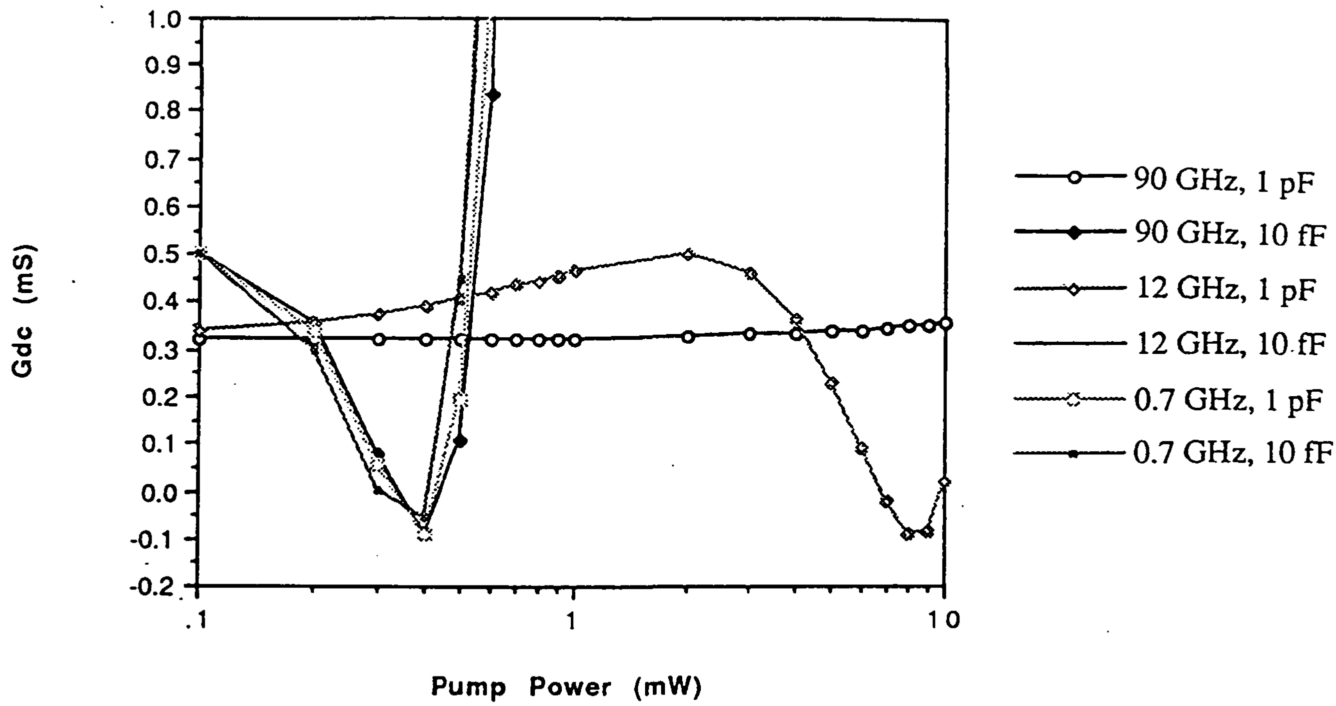
1.0
0.9
0.8
0.7
0.6
0.5
0.4
0.3
0.2
0.1
0.0
-0.1
-0.2
Gdc (mS)
.1
1
10
Pump Power (mW)
90 GHz, 1 pF
90 GHz, 10 fF
12 GHz, 1 pF
12 GHz, 10 fF
0.7 GHz, 1 pF
0.7 GHz, 10 fF

Fig. 5 (a)

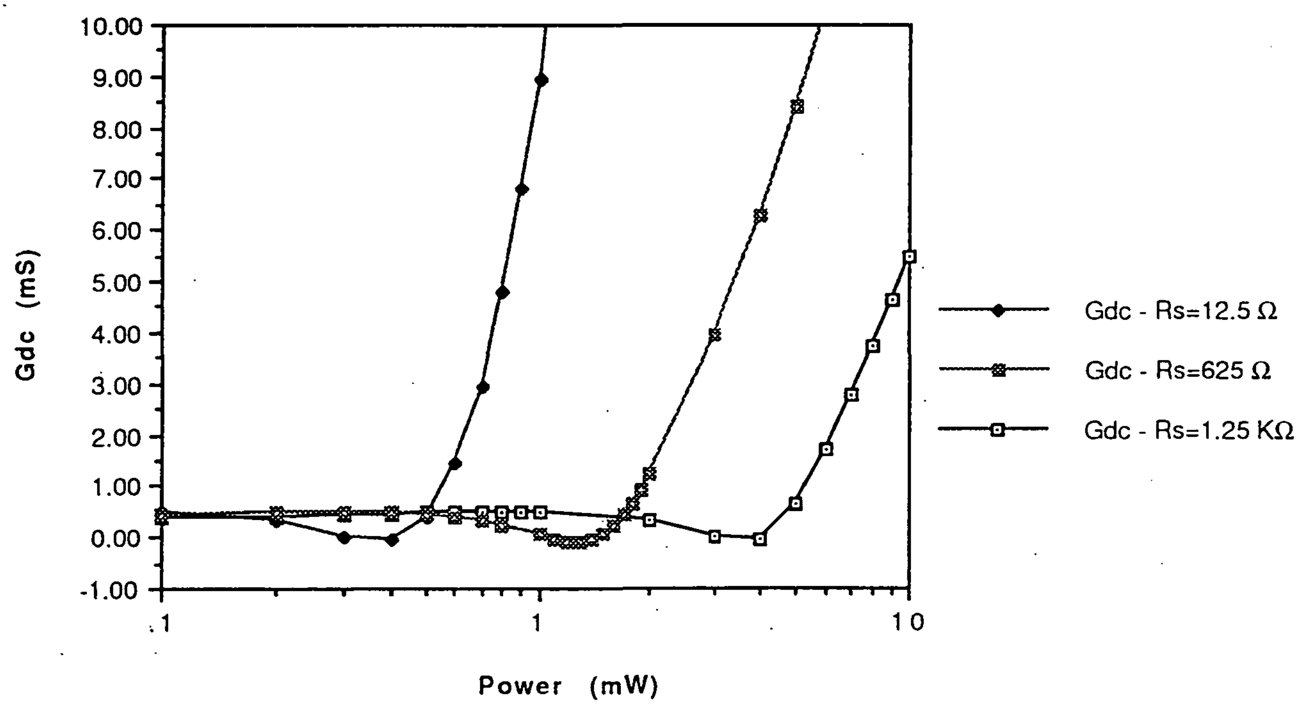
10.00
9.00
8.00
7.00
6.00
5.00
4.00
3.00
2.00
1.00
0.00
-1.00
Gdc (mS)
.1
1
10
Power (mW)
Gdc - Rs=12.5 Ω
Gdc - Rs=625 Ω
Gdc - Rs=1.25 KΩ

Fig. 5 (b)

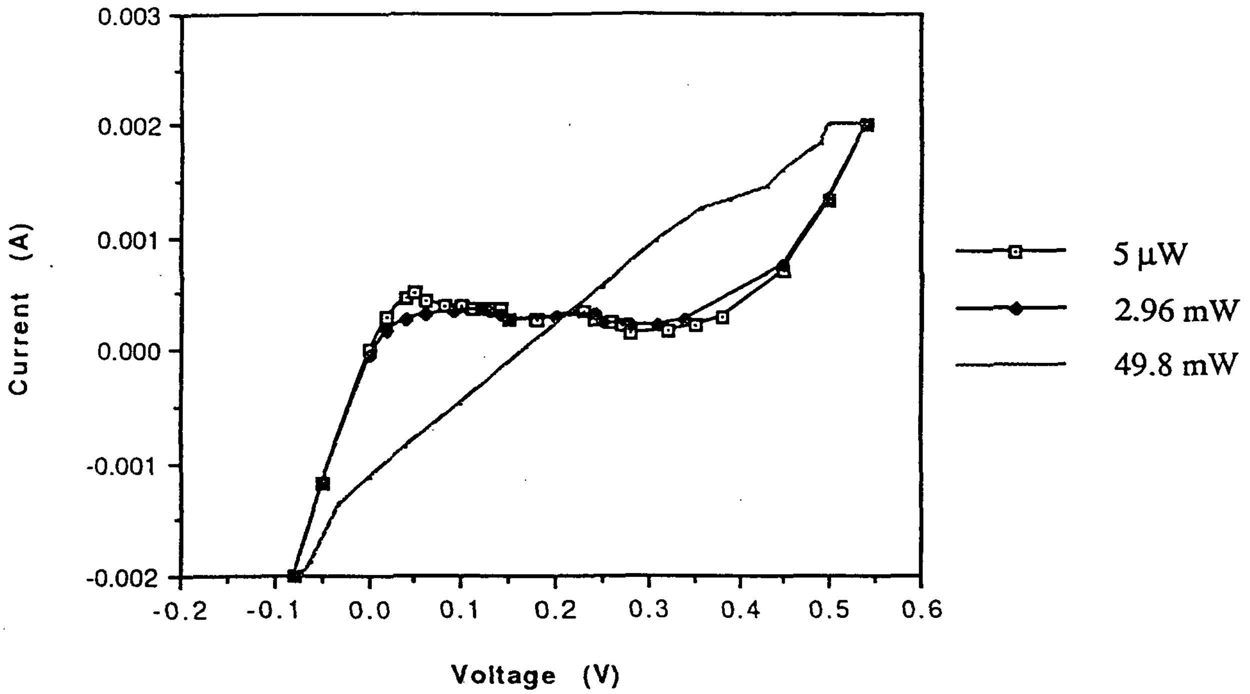

0.003
0.002
0.001
0.000
-0.001
-0.002
-0.2
-0.1
0.0
0.1
0.2
0.3
0.4
0.5
0.6
Current (A)
Voltage (V)
5 μW
2.96 mW
49.8 mW

Fig. 6 (a)

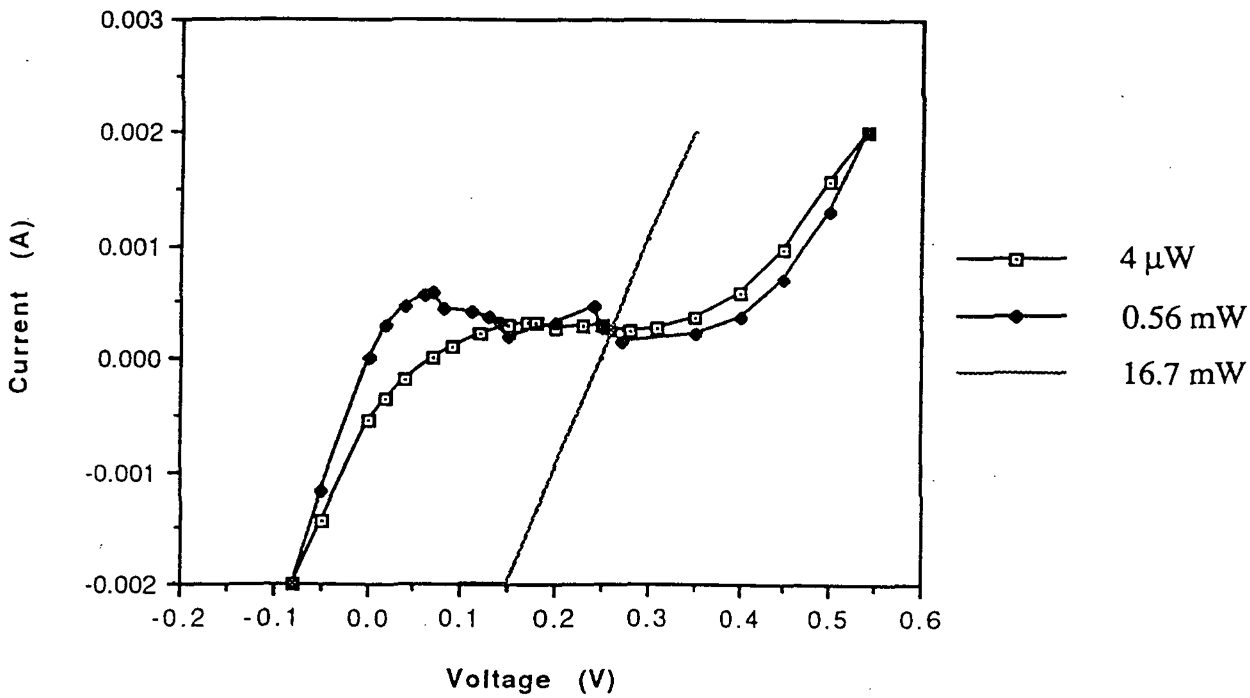

0.003
0.002
0.001
0.000
-0.001
-0.002
-0.2
-0.1
0.0
0.1
0.2
0.3
0.4
0.5
0.6
Current (A)
Voltage (V)
4 μW
0.56 mW
16.7 mW

Fig. 6 (b)

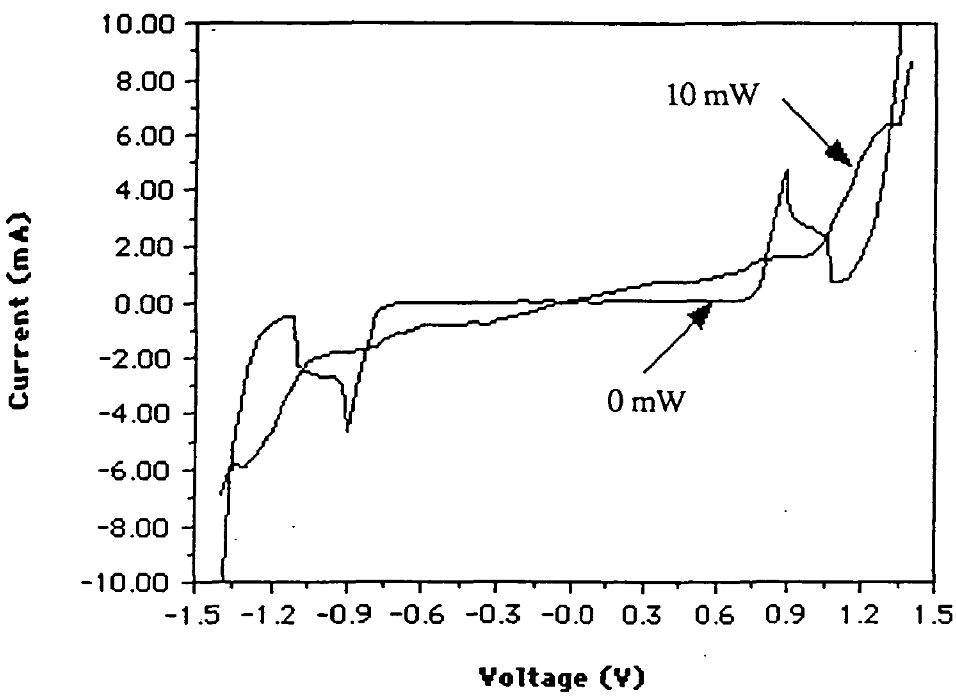

10.00
8.00
6.00
4.00
2.00
0.00
-2.00
-4.00
-6.00
-8.00
-10.00
Current (mA)
-1.5 -1.2 -0.9 -0.6 -0.3 -0.0 0.3 0.6 0.9 1.2 1.5
Voltage (V)
10 mW
0 mW

Fig. 7

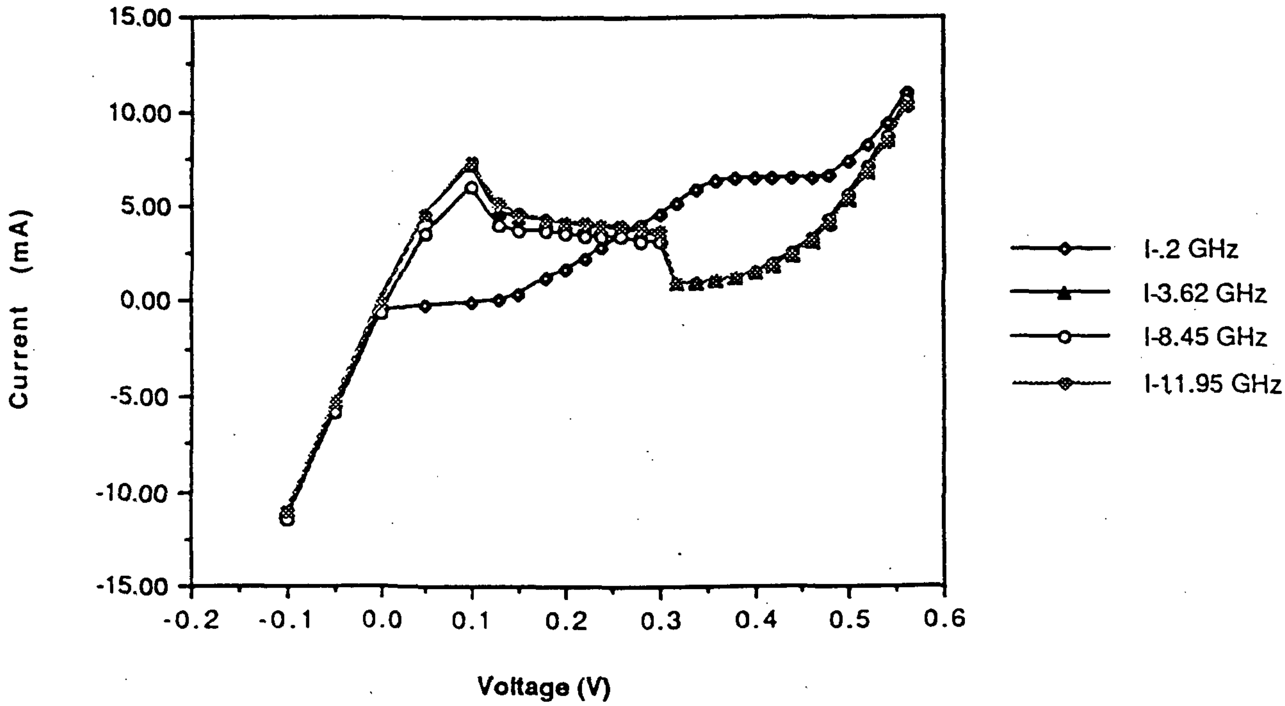
15.00
10.00
5.00
0.00
-5.00
-10.00
-15.00
Current (mA)
-0.2
-0.1
0.0
0.1
0.2
0.3
0.4
0.5
0.6
Voltage (V)
I-.2 GHz
I-3.62 GHz
I-8.45 GHz
I-11.95 GHz

Fig. 8

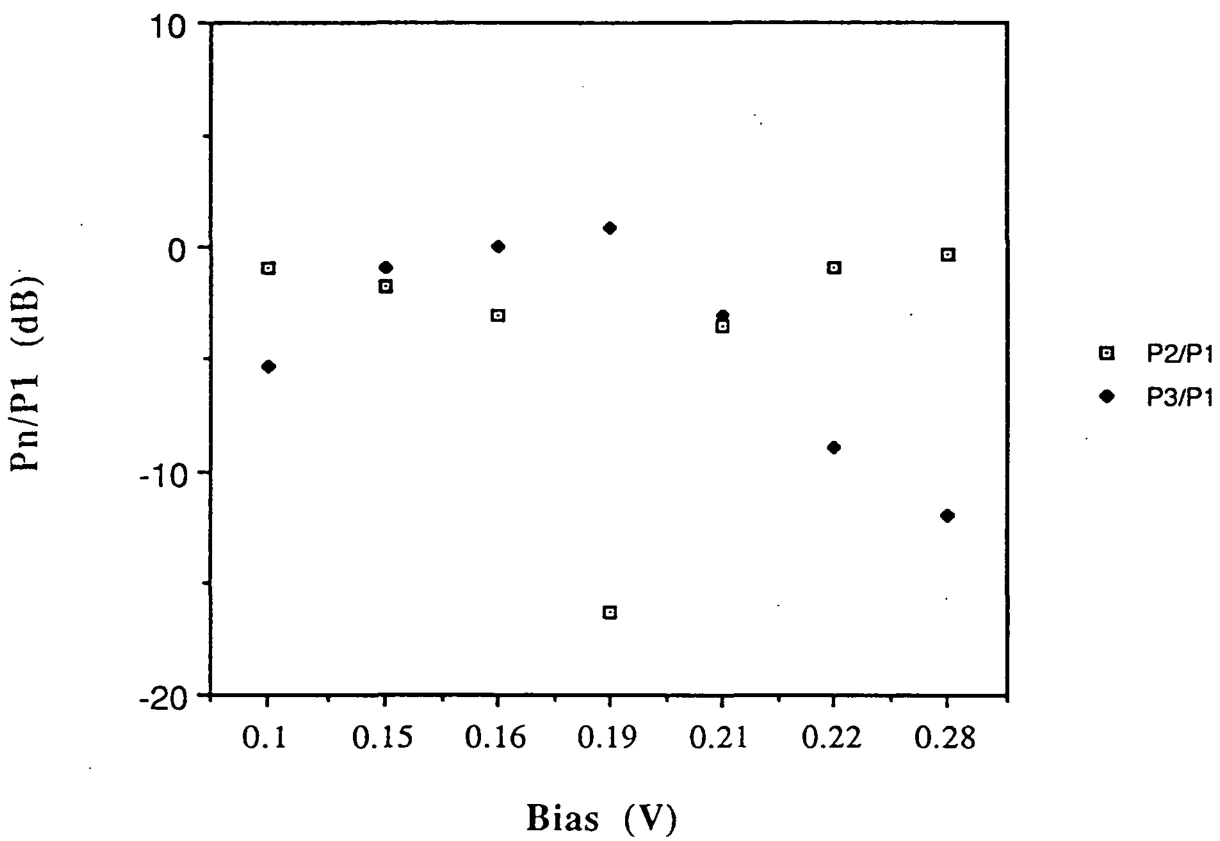

Fig. 9